

CFD Modelling of Erosive Wear

L CROCKER

JUNE 2014

CFD Modelling of Erosive Wear

Louise Crocker
Materials Division

SUMMARY

The wear process known as erosion occurs when discrete particles (e.g. solid particles or water droplets) strike a surface. The process causes surface damage, leading to material loss and mechanical degradation, potentially causing serious problems and economic loss. Material degradation is often unavoidable but the ability to model the erosion process allows engineers to improve component/system design through better material selection and the use of erosion reducing measures.

In this report, the use of Computational Fluid Dynamics (CFD) for modelling erosion will be reviewed. Using CFD, the movement of solid particles within a gas or liquid can be studied. Most detail is provided for the gas/solid particle combinations, although information on the liquid/solid particle combination is also included.

© Queens Printer and Controller of HMSO, 2014

ISSN 1754-2979

National Physical Laboratory
Hampton Road, Teddington, Middlesex, TW11 0LW

Extracts from this report may be reproduced provided the source is acknowledged and the extract is not taken out of context.

Approved on behalf of NPLML by Dr M Gee,
Knowledge Leader, Materials Team.

CONTENTS

1.	INTRODUCTION	1
2.	EROSION PROCESS	1
3.	EXPERIMENTAL	3
4.	MODELLING OF EROSIVE WEAR.....	3
4.1	GAS-SOLID TWO-PHASE MODELLING	4
4.1.1	Continuous flow field simulation	4
4.1.2	Particle Tracking	5
4.1.3	Erosion Prediction	9
4.1.4	Examples	12
4.2	FLUID-SOLID TWO-PHASE MODELLING.....	17
5.	CONCLUSIONS.....	24
6.	REFERENCES	24

1. INTRODUCTION

In industrial environments, wear can be a common problem. Within complex systems the in-service conditions are often demanding and various factors can influence the service life of components, potentially causing serious problems and economic loss.

The wear process known as erosion occurs when discrete particles (e.g. solid particles or water droplets) strike a surface. The presence of water droplets in the flow of a steam turbine, for example, leads to erosion of the moving blade. Similarly, sand within oil/gas pipelines can lead to pipe thinning. Erosion is a complex surface damage process, strongly affected by mechanical and metallurgical factors such as shape, size, density, hardness and quantity of erosive particles, particle velocity and angle of impact. The degree of degradation will also generally depend on the system characteristics e.g. pressure, temperature and type of erosive particles, and will also be strongly dependent on the materials used in the system.

The behaviour of the material being eroded will determine the erosion mechanism. For ductile metals material is removed through cutting and chip formation, while in brittle materials, material loss is due to crack formation and brittle fracture. Material degradation often cannot be avoided, but by selection of suitable materials and use of erosion reducing measures, a system fulfilling the requirements may be designed.

Many papers have been written on the experimental observations of erosive wear leading to a greater understanding of the mechanisms of erosion. Modelling of the erosion process naturally follows on from this experimental research. Modelling can be used to interpret existing experimental data, or to extend experimental data to conditions that cannot be tested with current facilities. Most significantly, modelling erosive wear can assist design engineers both in the design of better experimental test facilities for material characterisation and in the design of improved industrial components/systems. The long-term industrial aim is to develop a system where the components are manufactured from appropriate materials, the materials degradation modes are identified and that models exist to predict material performance [1]. Computational fluid dynamics (CFD) is often the modelling technique used to study the erosion process, and the aim of this report is to review current CFD methods for erosion modelling.

2. EROSION PROCESS

Bitter [2] described erosive wear as “Material damage caused by the attack of particles entrained in a fluid system impacting the surface at high speed”. Impacting solid or liquid particles carried within gas or fluid gradually remove material from the surface through repeated contact with the surface. Material removal due to repeated impacts can be concentrated at particular locations within a system due to geometry design and flow patterns within the system. The behaviour of materials when impacted by particles is very complex and depends on the material properties.

When the substrate surface behaves in a ductile manner, the impact of solid particles causes local plastic deformation at the impact site. Repeated impacts cause material loss as a result of a cutting or gouging action.

If the surface behaves in a brittle manner, the impact of the particles cause elastic deformation and crack formation. These cracks eventually link together and the material detaches from the surface.

The erosion rate of a material is dependent on impact angle amongst other factors. For brittle materials the mass loss increases progressively up to 90° impact [3], see Figure 1. For ductile materials the erosion rate (defined as the ratio of material mass loss to impacting particle mass)

reaches a peak at a lower impacting angle e.g. approximately 25° for steel, see Figure 2 [4], dropping off to zero at 90° . In practice, materials considered ductile will show mass loss at 90° impacts [3, 5]. It is suggested that this is as a result of work hardening due to repeated impacts, and high strain rates that produce fracture rather than plastic deformation [3].

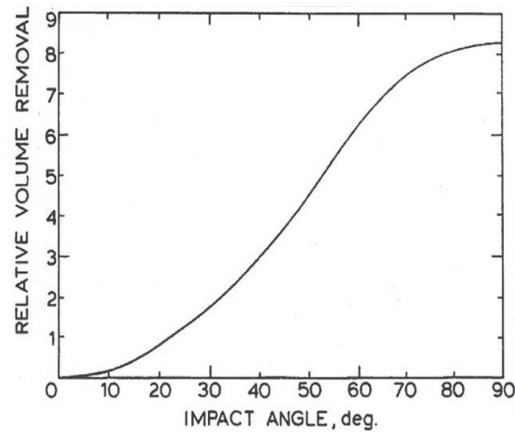


Figure 1. Theoretical curve for the relationship between volume removal and impact angle for a brittle material [3]

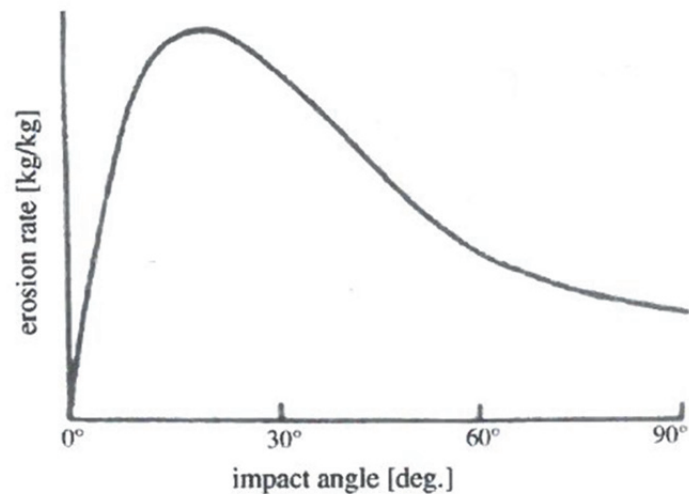


Figure 2. Theoretical curve for the relationship between erosion rate and impact angle for a ductile material [4]

A good understanding of the fundamental aspects of the particle impact erosion process, and the ability to predict erosion is of key importance for selection of appropriate materials and improved design of complex systems. While some of this understanding comes from studying plant data, much research has concentrated on lab-based studies using erosion rigs of various designs. With lab-based experiments, the factors influencing erosion are easier to control and measure, although it can be difficult to replicate real-world situations.

There are many factors that have an effect on erosion, for example:

- Substrate material properties
- Particle material properties
- Carrier gas/fluid behaviour
- Particle size distribution
- Particle shape
- Particle velocity
- Gas/liquid velocity
- Particle loading of gas/liquid
- Particle impact angle
- Particle impact velocity

The main problems in obtaining meaningful explanations of erosion data lie in the fact that variables are often inseparable and that a number of different mechanisms may be operating at the same time. In 1987, Bell and Rogers [3] suggested that a more detailed knowledge of particle interactions was required and that the most promising approach would be to model mathematically a combined fluid flow and particle system to calculate the results of particle interactions. In recent years this approach has been used by many researches to improve prediction of the erosion process, and is the main focus of this report.

3. EXPERIMENTAL

There is a wide range of experimental tests that are used for studying erosion. Typical examples of these are direct impingement tests and tests performed in flow loops. Direct impingement tests involve shooting particles e.g. sand or water particles, at a sample [6, 7]. The sample can be tilted to investigate the effect of impact angle on erosion. Velocity effects can also be studied. Flow loops are used to investigate the effects of geometry, particle size and fluid properties on erosion. Flow loops can be single phase (e.g. gas only) or multiphase (e.g. gas/liquid/sand) allowing a range of conditions to be tested [7-9]. To successfully study erosion, laboratory facilities must be able to replicate the particle loadings, velocities and temperatures experienced in the industrial system. The information obtained from these types of experiments has been used to develop a range of erosive wear models.

4. MODELLING OF EROSIVE WEAR

Due to the complexity of erosive wear it is not surprising that there is no universally accepted predictive model. However, a number of erosive wear models have been developed over the years. These range from the simpler single mechanism models, to the more rigorous models involving complex geometries/interactions.

Although erosion can occur in a wide range of situations, many models are industry/system specific e.g. water droplet erosion of turbines or solid particle erosion in pipelines. In many cases a fairly basic model will be used as a first pass assessment, to rank materials, followed by a more detailed model tailored to their requirements.

The simpler models are empirical models that use mass (or volume) loss equations to predict the erosion rate, and are often material specific. Mechanistic models can account for fluid and particle properties and flow rates. The more complicated models include Monte Carlo based solid particle erosion, finite element based models and computational fluid dynamics (CFD) based models.

CFD is a method particularly suited to predicting solid particle erosion inside pipe geometries or through nozzles. The technique is complicated and time consuming and, as such, is most appropriate for complex, non-standard geometries. The advantage of CFD is that it gives a quantitative insight into erosion dynamics both numerically and visually. It gives engineers the ability to modify designs rapidly and inexpensively.

Computational fluid dynamics is concerned with predicting fluid flow. The Lagrangian description of fluid flow focusses on fluid elements as they move through space and time, defined by using their original position and time as independent variables. The velocity and acceleration of a fluid element is readily derived through differentiation of the position vector with time. This Lagrangian analysis is rarely employed in single-phase flows [10]. The Eulerian description of a flow field focusses on specific locations in space through which the fluid flows as time passes. In this case velocity is the variable. Physical laws relate the dependent variables in a field and all flow properties are considered functions of spatial position and time [10]. The Reynolds number, Re , can be defined when a fluid moves relative to a surface. It is the ratio of inertial forces to viscous forces and is used to characterise flow regimes. Laminar flow has a low Reynolds number where viscous forces are dominant, giving smooth constant fluid motion. Turbulent flow has a high Reynolds number dominated by inertial forces, which tend to produce chaotic eddies and other flow instabilities.

Erosion, whether lab-based or in-service, generally involves two-phase flow: the motion of particles or droplets in a flow of gas or liquid. Both of these phases need to be modelled. The continuous flow phase is usually predicted from an Eulerian approach and the behaviour of the discrete particles is predicted from either an Eulerian or a Lagrangian approach. In an Eulerian-Eulerian approach a two-fluid flow of gas and particles is viewed as consisting of two interpenetrating continuous media [10], while the more common method is to use the Eulerian-Lagrangian approach, where the motion of individual particles can be tracked.

In two-phase flow, particle trajectories and impact will depend upon the fluid flow field. Particle velocity will vary as the flow field changes and, as the particle moves towards the target surface, its velocity magnitude and trajectory will depend upon the particle-fluid, particle-particle and particle-wall interactions [11]. The particle-fluid interactions depend upon the nature of the fluid flow regime, whether it is laminar or turbulent as well as the size, shape, relative density and motion of particles. The particle-particle interactions strongly depend on the concentration of the particles in the fluid phase. Particle-wall interactions depend on the surface topography and particle rebound characteristics of the system [12]

4.1 GAS-SOLID TWO-PHASE MODELLING

Gas-solid two-phase erosion modelling is a three step process:

1. Continuous carrier flow field simulation
2. Particle tracking using a Lagrangian approach (trajectory models)
3. Erosion calculation using information on particle impingements on the target surface

4.1.1 Continuous flow field simulation

CFD software is used to obtain a solution for the gas-particle flow. The flow is treated as the continuum phase and motion of this continuum phase is determined by solving the Reynolds-averaged Navier-Stokes (RANS) equations. The resulting flow field is a description of the velocity of the fluid at a given point in space and time. Navier-Stokes equations describe the motion of fluid based on conservation of momentum equations therefore other equations, such

as conservation of mass, conservation of energy, wall conditions, are also needed to define the flow field. The numerical solution of Navier-Stokes equations for turbulent flow is not possible, hence the use of the time-averaged, Reynolds-averaged Navier-Stokes equations supplemented with turbulence models to model turbulent flow in CFD.

CFD software packages, such as FLUENT, commonly use the finite volume method to discretize the continuity, momentum and energy equations [11-16]. A wall function is also required for near-wall treatment of the flow. The standard wall function is a no-slip condition at solid wall boundaries [14, 16, 17] although there are also enhanced wall functions [13]. 3D models are often used, due to the complex geometries being studied [4, 11, 13, 15, 16, 18] although 2D axisymmetric models can also be used [14].

The CFD method has an advantage in terms of memory usage and solution speed, especially for large problems and high Reynolds number turbulent flows. In this method, the governing partial differential equations (the Navier-Stokes equations, the mass and energy conservation equations and the turbulence equations) are recast in a conservative form and then solved over discrete control volumes. A solution algorithm often used is the SIMPLE method (semi implicit method for pressure linked equation) for 3D cascade flow field computation [4, 11, 16, 17].

Turbulence models are semi-empirical mathematical relations that can predict the general effect of turbulence. The k - ϵ turbulence model is the most common model used in CFD to simulate turbulent conditions. It is a two-equation model which gives a general description of turbulence through two transport equations (PDEs). The first transported variable determines the energy in the turbulence (turbulent kinetic energy, k). The second transported variable is the turbulent dissipation (ϵ) which determines the rate of dissipation of the turbulent kinetic energy. The underlying assumption is that turbulent viscosity is isotropic i.e. the ratio between Reynolds stress and mean rates of deformation is the same in all directions, although Atkinson *et al* [13] used a Reynolds stress model accounting for anisotropic turbulence. They found little difference to predictions from analyses with isotropic turbulence.

Although the standard k - ϵ turbulence model is often used [11, 14, 15], there are a range of other k - ϵ turbulence models available such as the RNG (Renormalization Group) based k - ϵ model; an extended version of the standard k - ϵ model; the realizable k - ϵ model and the low R_ϵ model. The standard k - ϵ model, RNG based k - ϵ model and extended k - ϵ model all use conventional logarithmic wall functions applied to wall-adjacent cells, and don't require a fine mesh near the walls [19]. The low- R_ϵ k - ϵ model uses a damping function to modify the turbulence parameters as the wall is approached. With this model a fine mesh is needed nearer the wall [19]. The realizable k - ϵ model can be used to evaluate the turbulent viscosity for high Reynolds flow [4]. El-Behery [17] studied gas-solid two-phase flow in a 180° curved U-bend using four of these models, comparing predicted data to measured energy data. All models over-predicted the turbulent kinetic energy, probably due to the use of isotropic turbulence models to predict anisotropic flow in the bend. In terms of the level and distribution of axial gas velocity, the RNG k - ϵ model performed best, with the standard k - ϵ model delivering poor results for this particular scenario.

4.1.2 Particle Tracking

The motion of particles within the continuous flow is usually modelled using a Lagrangian approach with each particle having its own starting point and particle size resulting in a series of trajectories throughout the computational domain [11]. It is known that the continuous flow field has an effect on the particle motion and vice versa. With CFD it is possible to couple the phases. One-way coupling is the simplest, with the lowest CPU cost and predicts particle paths as a post-process based on the flow field [20]. It has been suggested that this is an acceptable approach for dilute systems i.e. low particle concentrations and particle-particle interactions

assumed negligible [21, 22]. In most cases full coupling is used [11, 12, 15, 17, 23]. The basic premise is to compute the interphase exchange of momentum from the particle to the continuum phase by examining the change in momentum of a particle as it passes through each control volume in the computational domain i.e. the gas flow field is initially solved numerically as described in the previous section. The particle trajectories are then calculated through the gas flow field. The properties of the particles, on crossing the boundaries of the computation cells, yield the mass, momentum and energy terms for the gas in each cell. As mentioned, the geometry is divided into computational cells i.e. a mesh. A typical mesh is shown in Figure 3.

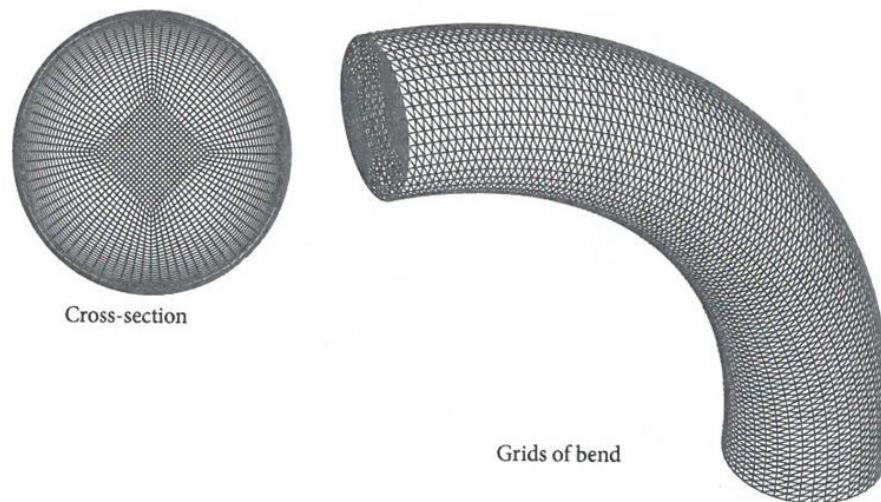


Figure 3. Typical mesh used on a pipe bend [16].

To predict the kinematics and trajectory of particles a discrete phase model (DPM) is often used [13-16]. The discrete phase model is a particle motion equation used to describe the turbulent properties of a discrete phase predicting the trajectory of particles and their impact angle and velocity. It includes the effect of instantaneous turbulent velocity fluctuations on the particle trajectory. The trajectory of a discrete particle can be predicted by integrating the force balance on the particle. This force balance equates the partial inertia with forces acting on the particle [15]. Full coupling is used and it includes a stochastic tracking model which predicts the dispersion of the particles. Particle size distribution also needs to be taken into account, for example, Gandhi *et al* [11] and Mbabazi and Shear [12] assumed the particle size distribution fitted the Rosin-Rammler equation. A large number of particle trajectories are required to gain a stochastically significant solution. A spherical drag law is often used in discrete phase modelling with two-way coupling between the particle and gas phase [11, 14].

When modelling two-phase flow, great care must be taken with the boundary conditions as these will strongly influence the predictions. A typical set of boundary conditions are given by Zhu *et al* [16]:

- Velocity of gas and particle are the same at the inlet with a uniform distribution
- After a certain distance it will form a fully developed flow
- Pressure outlet boundary conditions defined as 0 MPa
- No slip boundary condition on the inner wall

As well as modelling the trajectory of particle within the flow, the rebound/restitution behaviour also needs to be considered. The magnitude and direction of a particles rebounding velocity

depends upon the conditions at impact and the particular particle-surface material combination [24]. An example of a rebound model is shown in Figure 4 [4]:

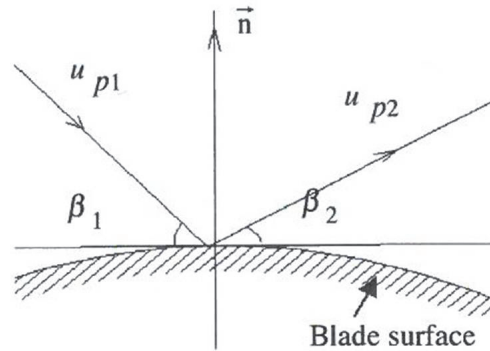


Figure 4. Schematic diagram of impact parameters for rebound model [4]

The ratio of particle rebound velocity to impacting velocity is u_{p1}/u_{p2} and the ratio of rebound angle to impacting angle is β_1/β_2 .

The restitution behaviour is a measure of the momentum lost by the particle at impact. When a particle impinges on a wall this energy loss must be taken into account to determine the reflected particle trajectory [22]. The energy lost corresponds with the work done on the target surface and thus influences the extent of erosive wear suffered by the material of the target surface. In some cases it is found that predicted wear rates differ from actual measurements. It is suggested that particle-particle interactions in experimental erosion lowers particle velocity resulting in much lower wear rates than those predicted [23].

The velocity coefficients of restitution depend upon the hardness of the target material, the density of the particle and the velocity at which the particle strikes the surface. In most cases simple restitution coefficients are assumed [4, 14], although in reality the situation is complex. In time, the target surface becomes pitted, changing local impact angles. If particles are irregular shapes with sharp corners, orientation has a large effect. Some particles cause little damage, while others can act as a cutting tool [24].

The two main methods for measuring the coefficient of restitution (COR) are high speed imaging and Laser Doppler Velocimetry (LDV). Reagle *et al* [18] used CFD in conjunction with Particle Tracking Velocimetry (PTV) to measure the coefficient of restitution. Using an aerothermal rig, pairs of images were captured and particle tracking software was used to determine velocities. Particles are tracked by correlating particles between frames, see Figure 5. The PTV particle data is combined with the CFD flow prediction. The impacting and rebounding velocities become a function of the measured particle velocity (from PTV), the flow field (from CFD), particle mass and particle size. Assuming a steady state flow field in front of the sample, the measured particle trajectories can be calculated forwards or backwards to yield velocities just before or after impact. COR, which is defined by the particle velocities just before and after impact, see equation 1, can be calculated.

$$COR = v_{reb}/v_{in} \quad (1)$$

Combining these two techniques to obtain COR means the advantages of each technique are maintained. CFD is good at particle tracking but not so good at particle impact/rebound while

PTV is good for finding impact velocities, but cannot continuously track particles at high speed due to hardware limitations. The results compare favourably with trends established in literature, see Figure 6. The experimental data shown in this figure are the closest experimental comparisons available in open literature for particle sand and ash at different impact angles.

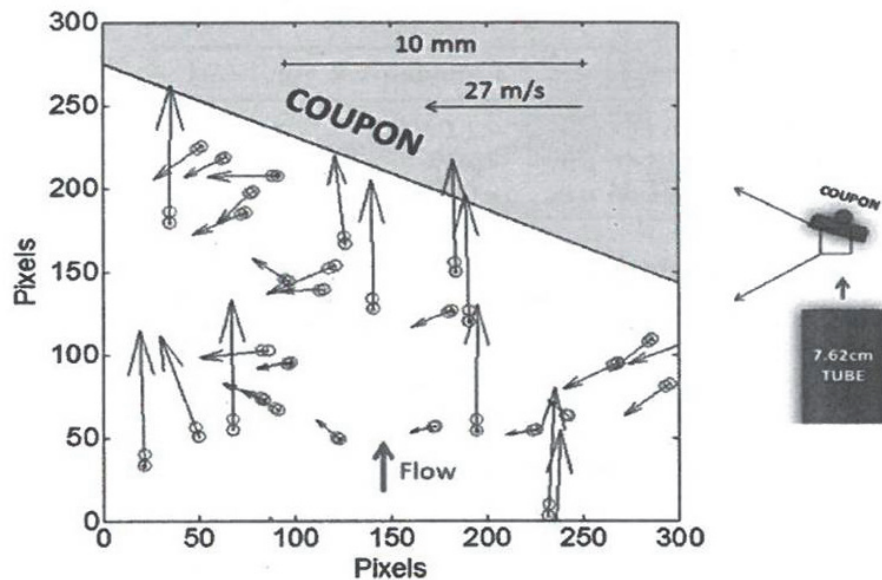


Figure 5. Particle tracking software results for 70° angle [18]

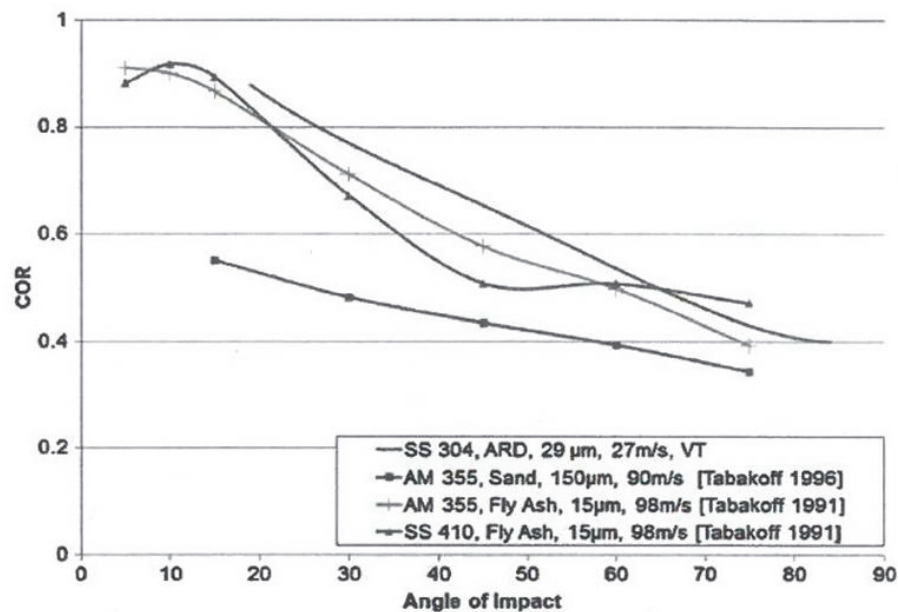


Figure 6. Comparison of calculated COR versus angle for Arizona road dust (ARD) with literature values [18]

The modelling of erosion is one of many engineering flow situations where particulate two-phase flows play an important role. The modelling approach outlined in this section and section 4.1.1 is suitable for many practical, non-erosion situations, such as spray drying [25-27] and micro abrasive blasting [28, 29]. The approach can also be extended to describe more complex situations such as four-phase flow with 2 immiscible liquids, gas and solid particles [30].

4.1.3 Erosion Prediction

CFD modelling allows impingement information, such as impact speed and angle, to be gathered as particles hit a surface. This information can be used as input into erosion equations to calculate erosion rates. The erosion equations are often incorporated into the CFD analysis as a user subroutine to enable the erosion rate to be determined directly from predicted impact velocities and angles.

The erosion rate, or erosion ratio, is defined as the ratio of mass loss of target material to impacting particle mass. A number of erosion models have been proposed over recent years. These are empirical in nature. In 1958 Finnie [31] proposed an erosion model based on a cutting mechanism, while Bitter [2, 32] (1963) proposed a wear and deformation model. Bitter's model is thought to be the most complete model but the number of material dependent constants needed make it nearly impossible to use in most practical situations. As a result, most commonly used models are based on Finnie's model.

Finnie predicted the erosion rate was:

$$E = \dot{m}v^n f(\alpha) \quad (2)$$

Where \dot{m} is the particle impact rate, v is the particle impact velocity, n is an empirical constant, α is the impact angle and f is a dimensionless wear function.

This equation has been modified by many authors, for instance Chen *et al* [22] used an equation of the form:

$$ER = AF_s V_0 f(\theta) \quad (3)$$

where ER is the erosion ratio, V_0 is the particle impingement velocity, A is a material dependent coefficient, F_s is a particle shape coefficient and $f(\theta)$ is a particle angle dependent function. Chen *et al* [22] then divide the erosion ratio by the pipe material density and local grid cell area to convert the erosion ratio to local wall thickness loss.

The erosion rate model is often correlated with experimental data to obtain constants. For example after studying experimentally obtained relationships of erosion rate to impacting velocity Dai *et al* [4] used an erosion equation of the form:

$$E = 2.12 \times 10^{-13} u_{p1}^{3.16} f(\beta_1) \quad (4)$$

where u_{p1} is impact velocity and β_1 is impact angle. Local penetration rates were calculated for each grid cell on the surface. Predicted maximum penetration rates were in good agreement with experimental data, see Figure 7, implying that the predicted distribution of particle impact angle and velocity were close to actual experimental conditions.

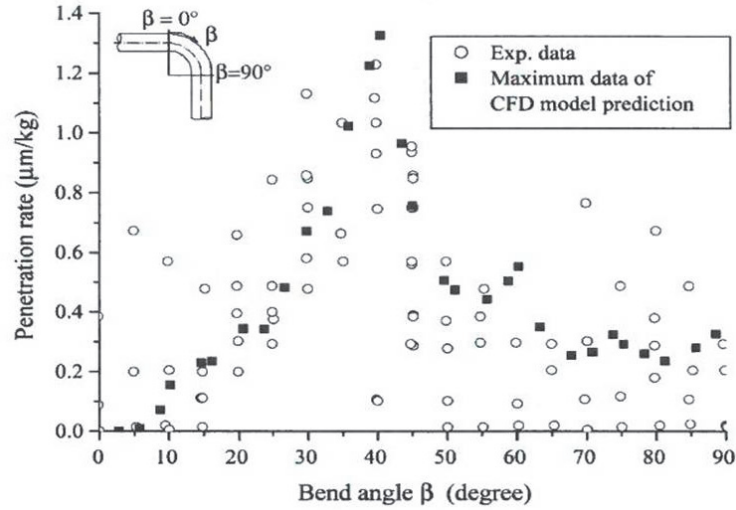


Figure 7. Comparison of predicted penetration rate with test data [4]

Hutchins [5] proposed an erosion model of the form:

$$E = \frac{K_1 \rho u^n f_1(\theta)}{H} \quad (5)$$

where K is the fraction of material removed as wear debris (wear coefficient), ρ is the density of the eroded material, u is the initial particle velocity, θ is the impact angle, f is the wear function, n is a velocity exponent and is a function of θ and H is the target surface hardness. This model is based on erosive wear by plastic deformation and is only valid for shallow angles of incidence as at higher angles the method of debris detachment changes.

Atkinson *et al* [13] used an erosion model based on Hutchins equation and fitted to experimental data, to calculate the erosion rate at every calculation point, enabling the generation of an erosion intensity surface map. They calculated weight loss by integrating the erosion rate intensity over the relevant areas, with good correlation between predicted and experimental weight loss.

Campos-Amezcu *et al* [15] used parameters calculated from a discrete phase model (DPM) to calculate the erosion rate, given as:

$$R_{erosion} = \sum_{p=1}^{N_{particle}} \frac{\dot{m}_p C(d_p) f(\alpha) v^{b(v)}}{A_{face}} \quad (6)$$

where \dot{m}_p is the mass flow rate of the particle stream, $C(d_p)$ is a function of the particle diameter, $f(\alpha)$ is a function of the impact angle of the particle with the wall, v is the relative particle impact velocity, $b(v)$ is a function of the relative particle velocity and A_{face} is the area of the cell wall. The impact angle function was defined by a piece-wise linear profile.

A similar model, again based on a DPM model, was used by Zhu *et al* [16], with the erosion rate determined by mass transfer:

$$e = \sum_{s=1}^{N_s} \frac{1.8 \times 10^{-9} M_s}{A} \quad (7)$$

where M_s is the mass rate and N_s is the number of particles. A is the projected area of particles at the wall.

Mbabazi *et al* [24] used experimental data of boiler fly ash particles impacting mild steel to calibrate a fundamentally derived model for the prediction of erosion rates. The equation uses all major parameters responsible for metal erosion, including yield stress of the steel and fly ash properties. The erosion rate equation is given as:

$$E(I) = \frac{Kx^{4.95}\rho_m\rho_p^{1/2}V^3(I)\sin^3\beta(I)}{\sigma_y^{3/2}} \quad (8)$$

The model was used by the authors as a fortran subroutine to investigate the effect of different types of ash particles with varying silica contents, where the predicted results differed by less than 15% from experimentally measured values, and to predict erosion of air heater elements (where the majority of results were not more than 10% from measured values) [12].

This model was also used by other authors such as Gandhi *et al* [11] who used it to predict erosion rates in large scale wall-fired boilers to identify areas of the furnace which may be more prone to erosion. There was reasonable agreement between predicted and experimental values, see Figure 8.

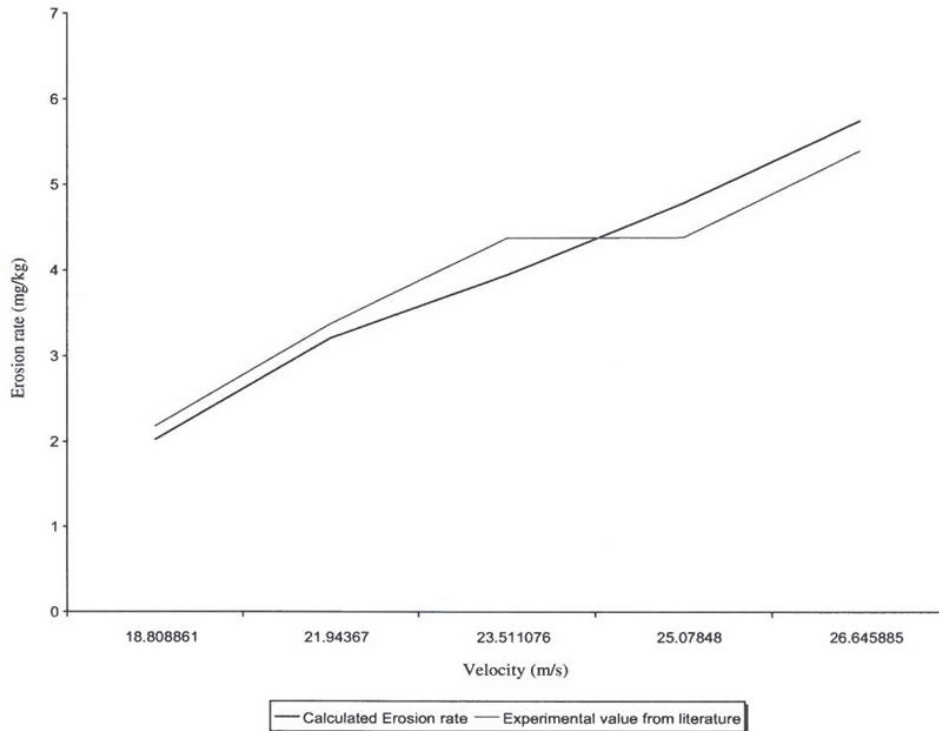


Figure 8. Comparison between calculated erosion rates with experimental data at a constant impingement angle of 30° for different velocities [11].

There are situations where erosion occurs on a stand-alone surface rather than, for example, the inner surface of a pipe or tube. Examples of this are erosion testing, shot peening and blast cleaning applications, where particles are ejected from a nozzle as a diverging plume. In order to model erosion of a target surface, the distribution of particles on nozzle exit (the plume

shape) needs to be included. The plume shape has been defined mathematically by Shipway and Hutchings [33] who studied the particle distribution and velocities experimentally. A computer simulation of this has been presented by Papini *et al* [34] and compared to the experimental data of Shipway and Hutchings [33]. The model includes the effect of angle of incidence, nozzle parameters, particle velocity and distribution, particle size, particle-particle and particle-surface impact parameters, nozzle stand-off distance and incident particle flux. The authors were particularly interested in the extent of particle interference between incident and rebounding spheres. In order to avoid falsely attributing the results of erosion tests to incident particle parameters when in reality they might be due to interference between incident and rebounding particles it is suggested that experiments should be performed at a low enough critical flux that interference effects are negligible. The model was used alongside a minimal number of scar radius experiments to determine this critical flux.

4.1.4 Examples

The methodology for predicting erosion rates using CFD are fairly well established, with the main differences being selection of one-way coupling/full coupling of Eulerian/Lagrangian analyses, choice of particle tracking model and erosion rate equation used. This methodology can be used for a wide variety of different situations. It is particularly useful for comparing the relative erosion rates of different geometries. The ability to vary parameters quickly and easily in a CFD analysis can be used to fine tune single component design or to investigate the effect of change in operating conditions.

Mbabazi and Shear [12] modelled seven different plate element profiles to investigate how erosion varies with element geometry under the operational conditions for a power station in South Africa. The model included rotation of air at 0.6 rpm corresponding to operation conditions for air heaters. The effect of plate geometry alignment with regard to flow direction was of particular interest. Initially the validity of the erosion model was confirmed by comparing specific CFD simulations with results from experimental investigations. Subsequent CFD simulations showed that the geometry of the air heater element had significant influence on the erosion rates and hence service lives. Very low erosion rates were found for elements aligned to flow directions while much higher erosion rates were predicted for plates at an angle to the flow. This is shown in Figure 9, where low erosion rates are predicted for the air heater elements labelled NF6 and K8G, which are aligned with the flow direction.

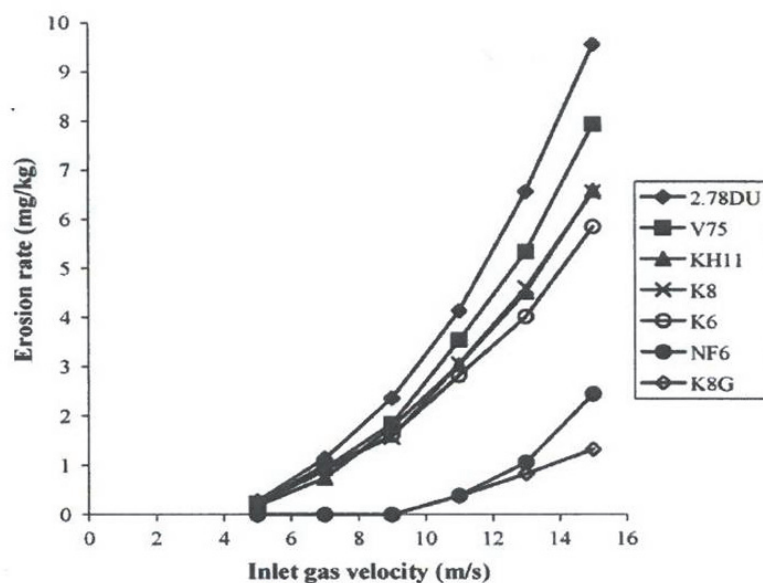


Figure 9. Predicted erosion rates for different air heater elements [12]

Atkinson *et al* [13] investigated sand erosion in 3D flow channels. An accelerated laboratory testing approach was developed to measure erosion in complicated 3D configurations. This experimental data was used to validate the CFD models. CFD was capable of predicting the fine details of the initial erosion pattern, see Figure 10. As erosion developed further, the details faded but were still distinguishable. For the CFD analysis, weight loss was calculated by integrating the erosion rate intensity over the relevant areas. There was good correlation between predicted and measured weight loss, see Table 1.

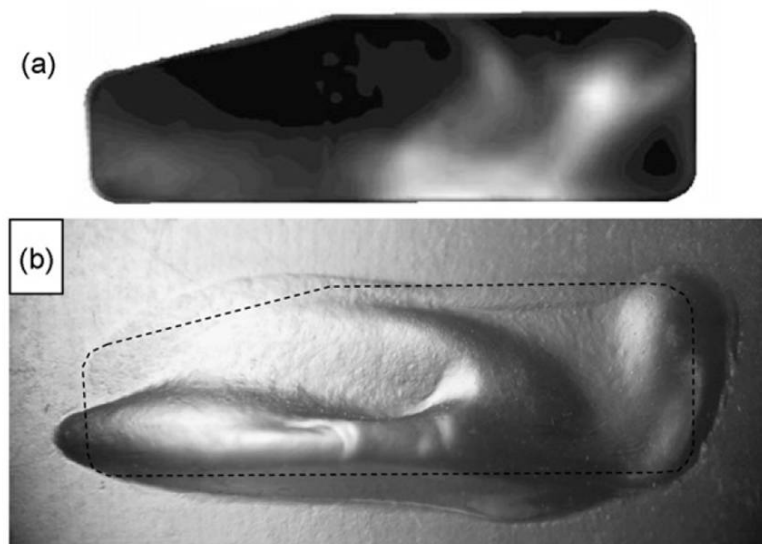


Figure 10. CFD predicted erosion intensity (a) and experimental erosion pattern on the lower plate of the flow channel [13]

Table 1. Comparison of actual weight losses in the plate specimens with CFD predictions [13]

Plate no.	Predicted weight loss (mg/g)	Measured weight loss (mg/g)
Channel A, 47 g of silica sand used		
1	0.98	0.94
2	4.29	4.62
3	1.29	1.96
Channel B, 52 g of silica sand used		
1	0.53	0.59
2	0.86	0.56
3	1.17	1.32
4	0.86	0.96
5	0.53	0.68
Channel C, 57 g of silica sand used		
1	0.02	0.09
2	0.45	0.33
3	3.81	2.59

Chen *et al* [22] studied the difference between plugged tees and elbows. Plugged tees are often used in industry to replace elbows when erosion is expected though it is unclear whether plugged tees reduce erosion. Analysis of CFD model predictions and experimental observations of the tee and elbow geometries highlighted that particle recirculation is an issue in plugged tees as shown in Figure 11.

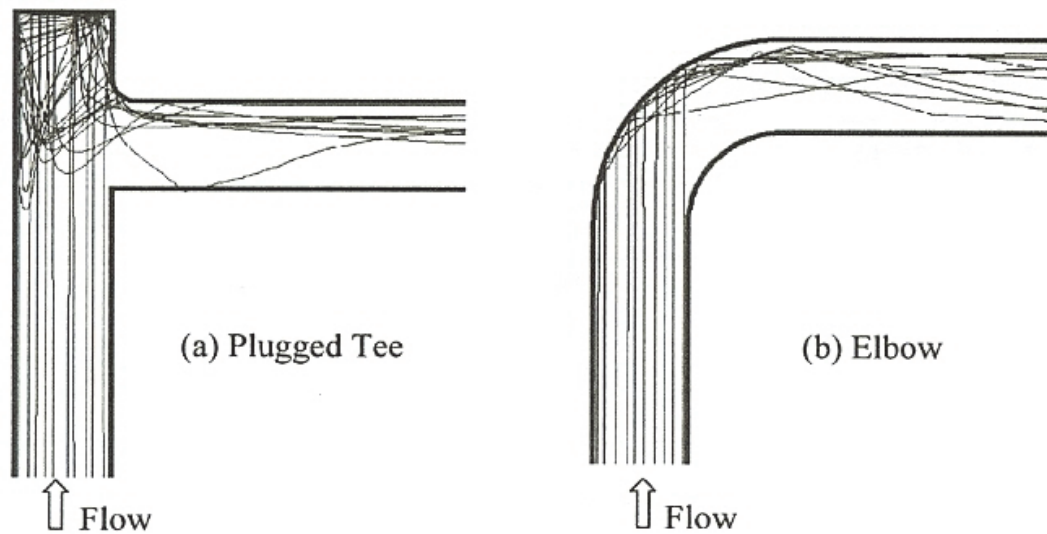


Figure 11. CFD predicted particle trajectories in the plugged tee and elbow geometries [22]

When comparing with experimental data, good agreement was found for large particle diameters ($> 150 \mu\text{m}$) but with smaller diameters the particle recirculation is numerically exaggerated resulting in over prediction of erosion. This was compensated for by separating out the first impingement of particles and subsequent impingement due to recirculation. This is demonstrated in Figure 12, which compares measured and predicted relative erosion rates for two different regions. Erosion at the corner (Figure 12b) is primarily caused by the first impingement of particles, thus the predictions of Figure 12b are free of the numerical discrepancy of particle recirculation that is included in Figure 12a.

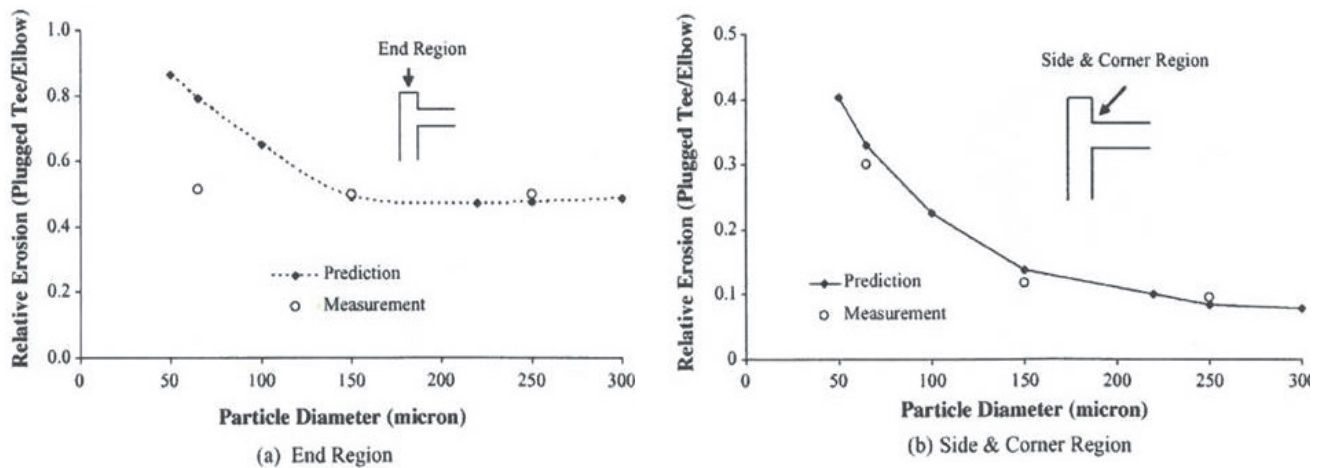


Figure 12. Predicted and measured relative erosion between the plugged tee and the elbow [22]

Dai *et al* [4] used CFD to study the anti-erosion performance of control stage nozzles of supercritical stream turbines which can be prone to solid particle erosion. Two alternative nozzle designs, one with a contoured endwall, the other an aft-loaded nozzle, were compared with a standard straight endwall nozzle. CFD analysis showed clearly that the contoured endwall design markedly reduced the erosion on the pressure surface, while in the case of the aft-loaded nozzle design, erosion was actually more severe, See Figures 13-15.

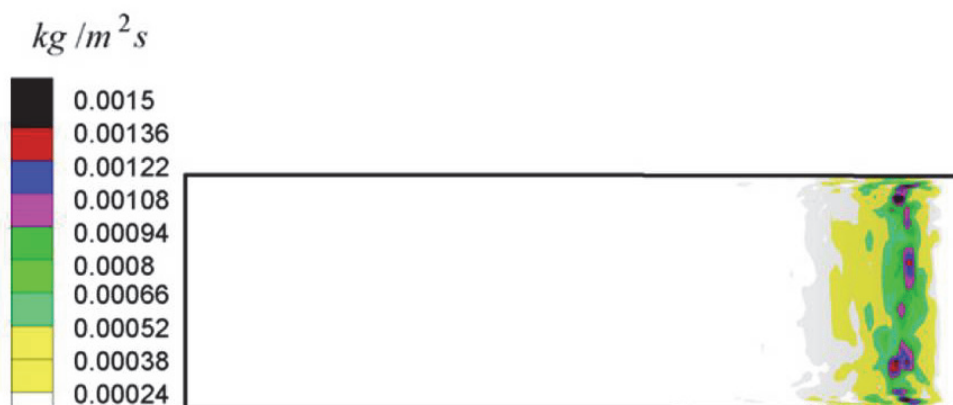


Figure 13. Local erosion rate distribution on the pressure surface of the straight endwall nozzle [4]

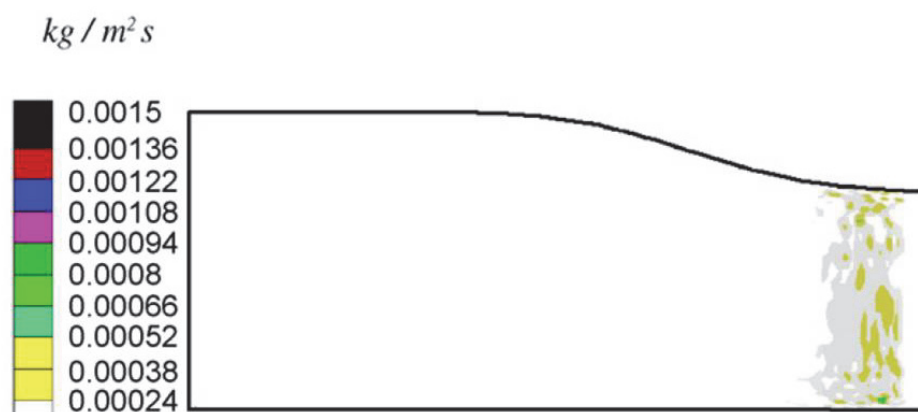


Figure 14. Local erosion rate distribution on the pressure surface of the endwall contouring nozzle [4]

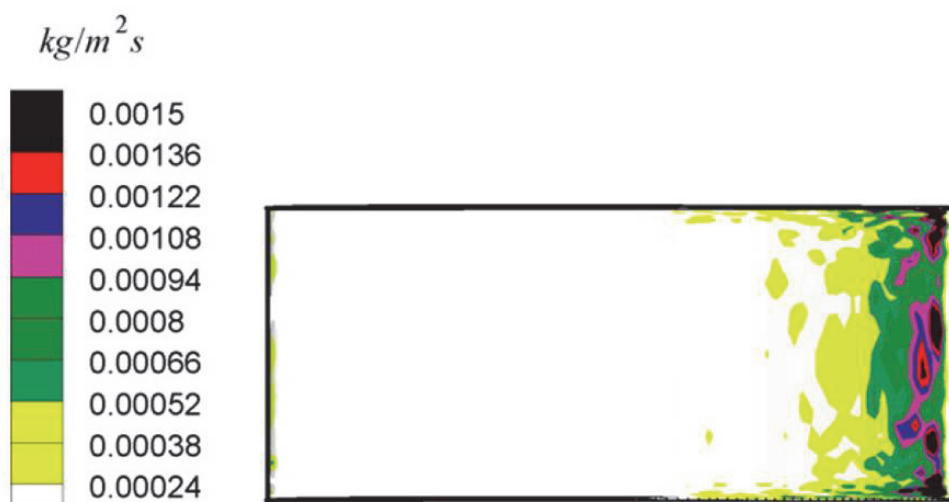


Figure 15. Local erosion rate distribution on the pressure surface of aft-loaded nozzle [4]

Campos-Amezcuca *et al* [15] also modelled the erosion of steam turbine nozzles (stationary control stage) but used CFD to predict the effects of operational changes. Results showed that within the operational ranges studied, solid mass flow rate had more effect on the erosion rate than steam mass flow rate, and that the maximum erosion rate decreased slightly with increasing particle diameter, see Figure 16.

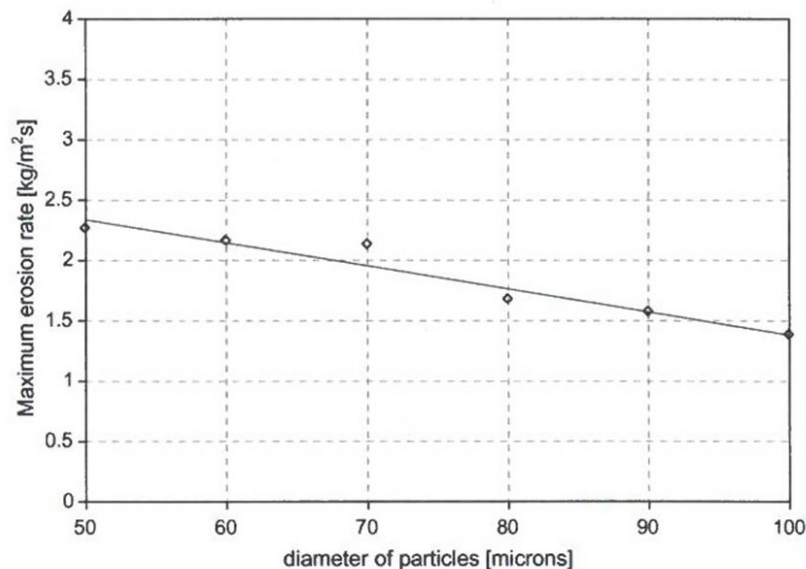


Figure 16. Maximum erosion rate versus diameter of the particles [15]

The effect of varying parameters such as inlet gas velocity, particle diameter, curvature ratio and mass loading ratio etc of flow in pipes can be investigated using CFD [16, 17]. For instance Zhu *et al* [16] found that in pipes, erosion rate was sensitive to inlet velocity, pipe diameter, bend curvature, sand volume fraction and particle diameter and demonstrated that reducing flow rate, sand concentration or particle size would reduce erosion rates.

A key factor to validating any relationships/effects observed from CFD analysis is to have experimental data for comparison. Lab-based data is particularly useful for validating models as conditions can be more closely controlled than in plant. CFD often plays a significant role in the design of erosion test-rigs. An overview of the process used to design a burner rig for studying erosion of TBC's has been presented by Kuczmarski *et al* [14]. Their model demonstrated that the major conditions necessary: namely particles to reach gas temperature; particles to move fast enough to cause damage and ability to broaden eroded region when necessary, could be achieved with 26 μm diameter particles. The size of the eroded region is determined by the stand-off distance between nozzle and sample and the distribution of particle velocities and trajectories in the plume of erodent leaving the nozzle [33]. The model was validated with data from the actual rig and showed good comparisons of temperatures and velocities. By studying the most probable particle trajectories it was predicted that most particle strikes would occur below the centreline of the sample, and this was confirmed experimentally, see Figure 17.

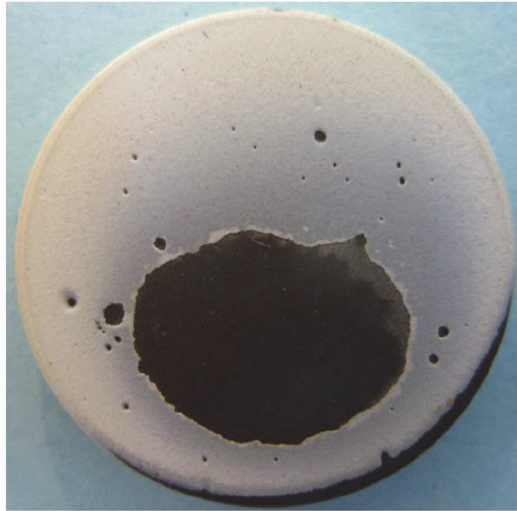


Figure 17. Experimental observation of eroded pattern on test sample [33]

4.2 FLUID-SOLID TWO-PHASE MODELLING

Sand is commonly found entrained in water (i.e. slurry) within pipes in the oil and gas industry. These sand particles can cause extensive erosion damage. The behaviour of particles in fluid is known to be different to that in air [35]. For particles within a fluid the particle velocity may not be the same as the liquid velocity, and the particle paths can vary significantly from the carrier fluid path, whereas in gas the particle speed and impact angle is similar to that of the gas.

Despite these differences, the general methodology for modelling fluid-particle behaviour is consistent with that for predicting gas-particle behaviour i.e.

1. Calculate fluid velocity field
2. Calculate particle trajectories, impact rate, angle and velocity
3. Apply erosion model to calculate erosion rate

Erosion is influenced by sand characteristics (concentration, impact velocity and angle, number of impacts, shape and size distribution), component geometry and material properties (hardness, microstructure, ductility) and also the fluid characteristics (flow rate, composition, density and viscosity). Either one-way coupling [19-21] or full-coupling [36, 37] between the fluid and particle phases is used. It is often assumed that the solid particle concentration is very low and solid particles do not affect the velocity of the fluids [35, 36].

Once again Eulerian-Lagrangian formulations are commonly used to model the complex water-sand combination along with the turbulence (k- ϵ) models and wall functions described in Section 4.1.1. These are often used with a stochastic dispersion model to calculate the influence of liquid phase turbulence on the solid particle phase [37], although alternative models are also available. Willis *et al* [38] used an algebraic slip model. When sand is in suspension the sand does not simply follow the movement of the water but is strongly influenced by it. The algebraic slip model appreciates that the water and sand have different velocities. The model solves a single velocity vector, but the separate velocity fields for sand and water are available, so sand doesn't have to follow the fluid streamlines.

Using data obtained from the particle tracking simulations, erosion rates can be calculated. Once again, many of the erosion equations used are based on Finnie's model [19-21, 39], see section 4.1.3, although Lester *et al* [40] suggested this simple form of equation was not suitable; instead developing a model that included a general fitting function for velocity dependence to improve results. Zhang *et al* [35] investigated various erosion models including the Erosion-Corrosion Research Centre (E/CRC) model for carbon steel. This model includes surface material properties and is given as:

$$ER = C(BH)^{-0.59} F_s V_p^n F(\theta) \quad (9)$$

where

$$F(\theta) = \sum_{i=1}^5 A_i \theta^i \quad (10)$$

ER is the erosion rate, BH is the Brinell hardness of the wall material, F_s is the particle shape coefficient, V_p is the particle impact speed, θ is the particle shape coefficient and A_i , n and C are empirical constants. This model predicted erosion rates in direct impact tests that compared reasonably well with measured data.

Azimian and Bart [37] used the Grant and Tabakoff erosion equation to model a slurry tank test rig. This model takes into account both the incoming and rebounding particle velocities:

$$E = k_1 f(\beta_1)(V_{1T}^2 - V_{2T}^2) + F(V_{1N}) \quad (11)$$

Where k_1 is a material constant, $f(\beta_1)$ is the empirical function of particle impact angle, V_{1T} and V_{2T} are the tangential component of incoming particle velocity and rebounding particle velocity respectively and $F(V_{1N})$ is the component of erosion due to the normal component of velocity. This was used to predict material weight loss at various sand concentrations and correlated reasonably well with experimental data, see Figure 18.

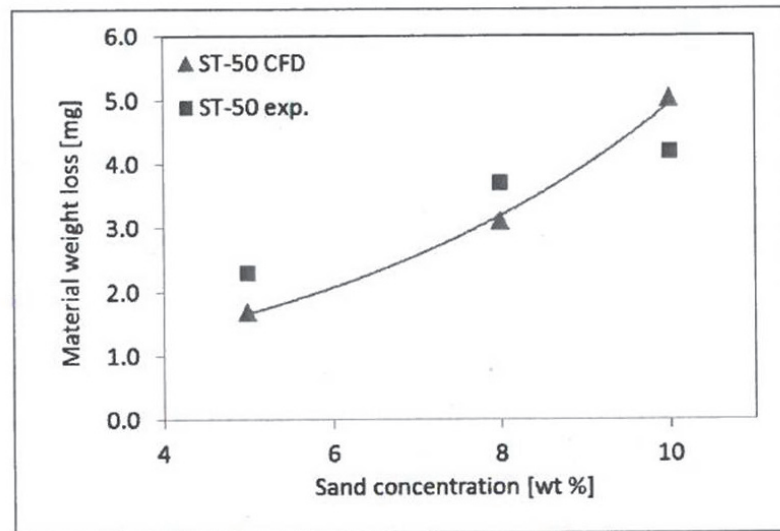


Figure 18. Validation of CFD and experimental erosion results for various sand concentrations [37]

An alternative erosion prediction method has been presented by Gnanavelu *et al* [36] who have generated wear maps for specific material/erodent combinations. A set of carefully controlled erosion tests were carried out to obtain local wear rates. CFD simulations of tests under exact

conditions provided local particle impact data (velocity, angle, rate). This data was used to generate a universal wear map giving wear/impact as a function of local particle impact velocity and angle for the specific material/erodent combination. A CFD simulation of a complex geometry can then be run giving impact velocity, angle and frequency at each position within the geometry. The generated wear map can be used to predict the local wear rate at each point. A comparison between the erosion ratios for the wear map method, predicted using a combined Finnie-Bitter model, and experimental data are shown in Figure 19. For the wear map method, the variation of erosion ratio with position on the sample follows the same trend as the experimental data.

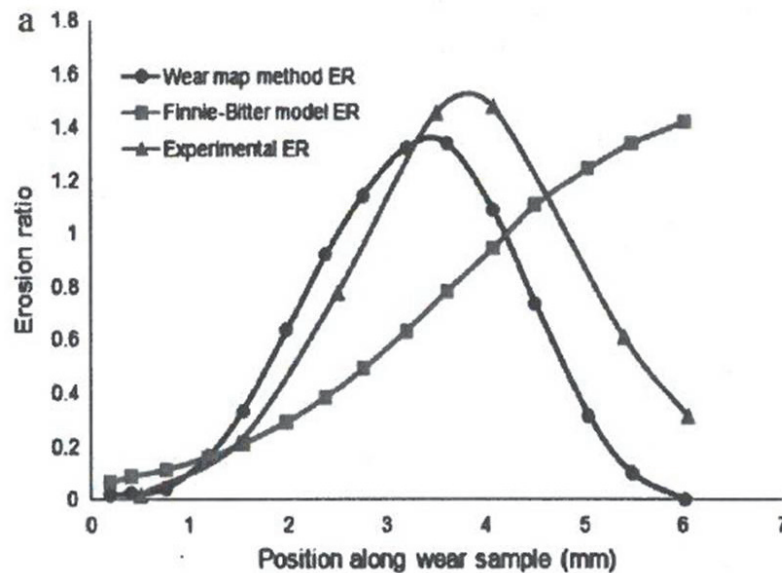


Figure 19. A comparison of the erosion ratio for the wear map method, a combined Finnie-Bitter model and experimental data [36]

The erosion models used often need parameters determined from experimental data. It is also useful to have experimental results to compare CFD predictions with. Lester *et al* [40] cautioned that when running CFD analyses you should not extrapolate outside the envelope of experimental data. The validity of the CFD approach has been demonstrated by Zhang *et al* [35] by measuring the velocity of particles entrained in water approaching a target using Laser Doppler Velocimetry (LDV). CFD simulations of the experiments were carried out and were found to match the data very well for fluid and particle velocities and impact speeds demonstrating the CFD is a viable method for predicting these parameters, see Figures 20-22.

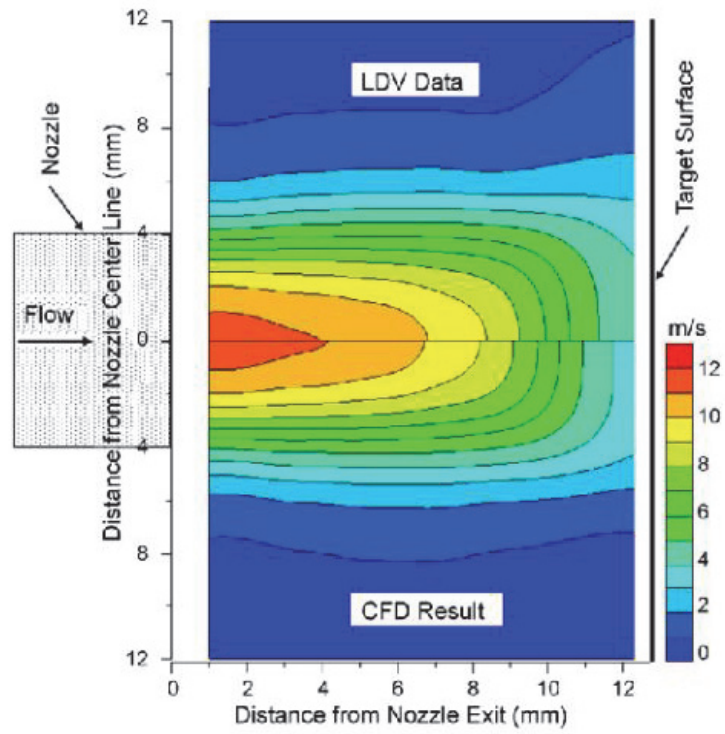


Figure 20. Axial fluid velocity, LDV data versus CFD result [35]

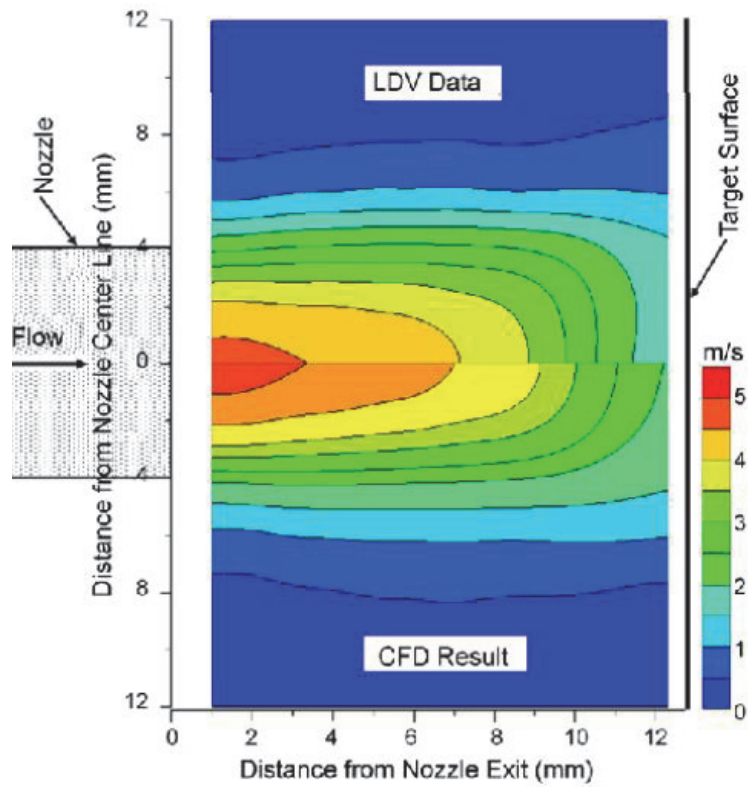


Figure 21. Axial particle velocity, LDV data versus CFD result [35]

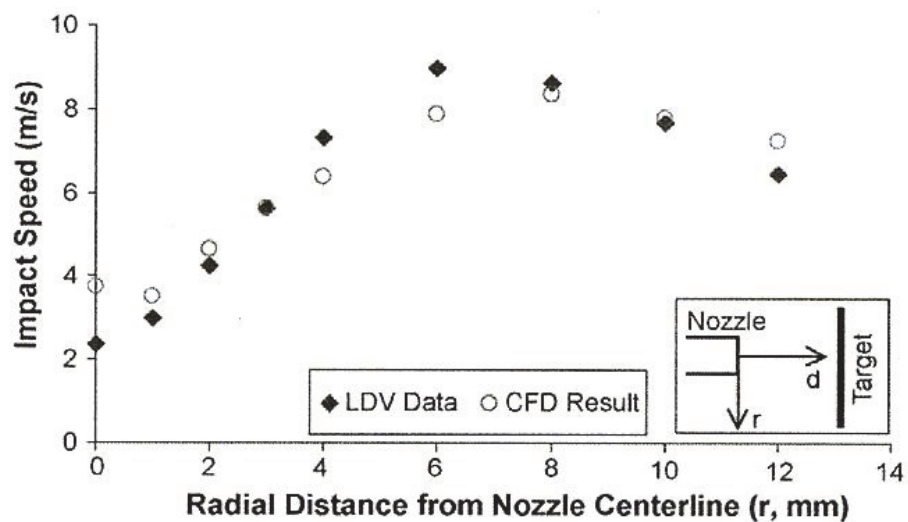


Figure 22. Particle impact speed, LDV data versus CFD result [35]

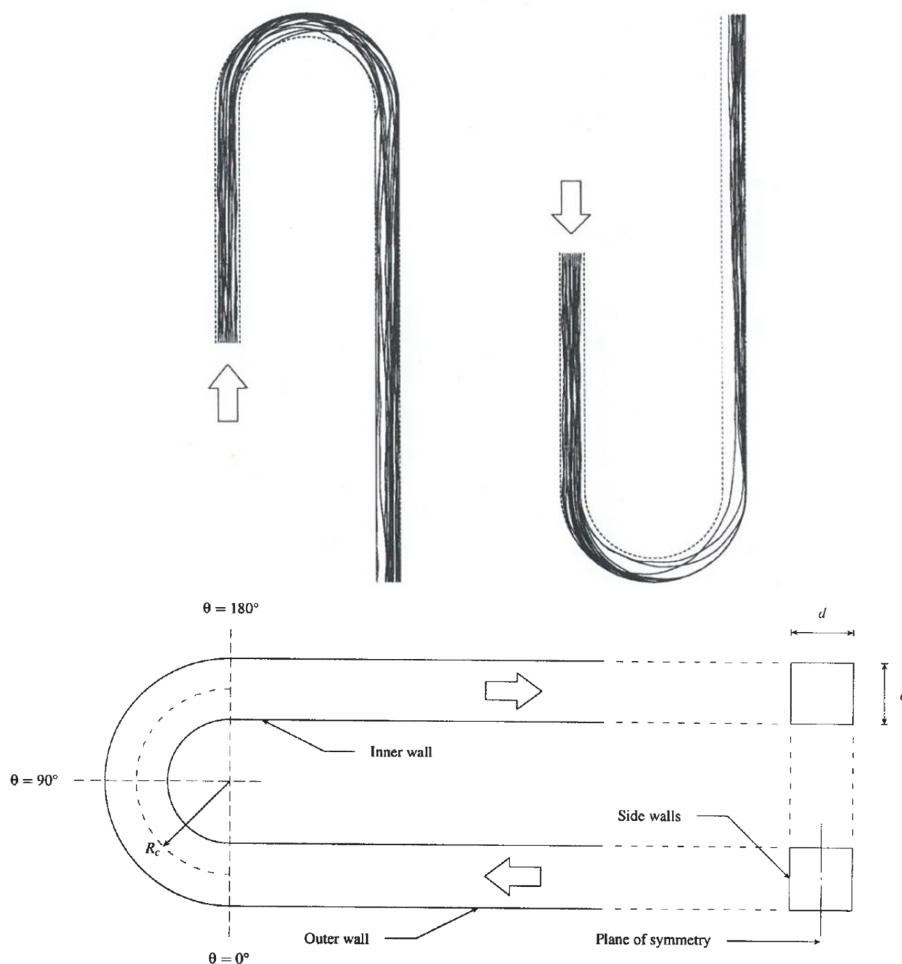


Figure 23. Schematic of a U bend and Sample particle trajectories for upward and downward facing U bends [21]

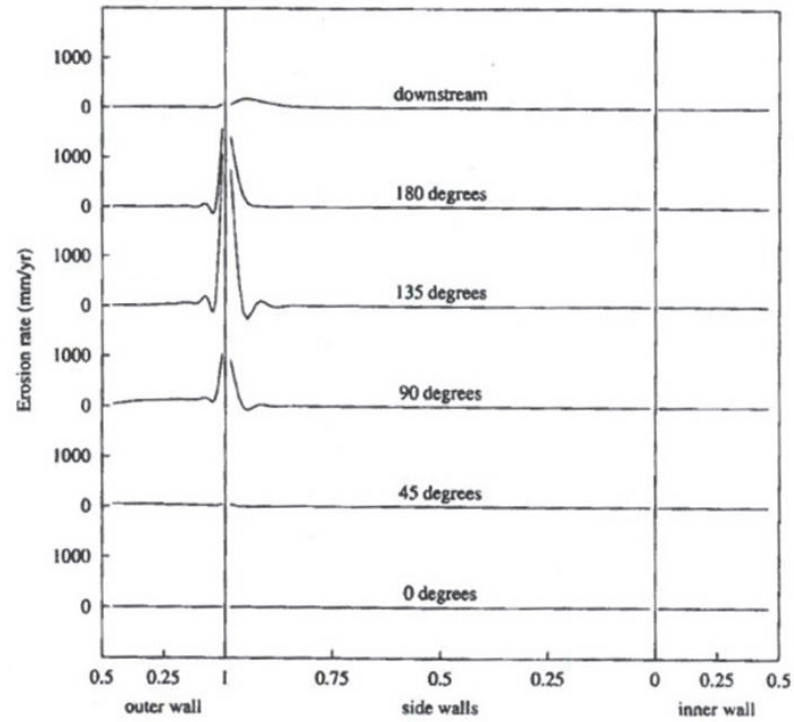


Figure 24. Predicted erosion rate for sand particles on the outer, side and inner walls of an upward facing U bend [21]

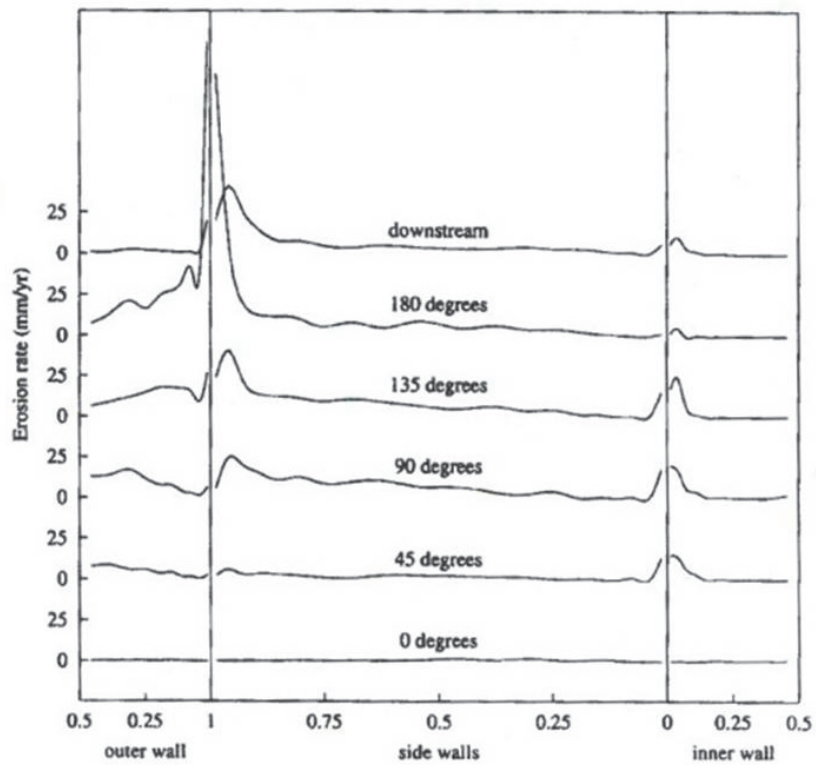


Figure 25. Predicted erosion rate for sand particles on the outer, side and inner walls of a downward facing U bend [21]

In the absence of experimental data, CFD can provide probable particle trajectories and erosion rate predictions. For example Keating and Nesic [21] used CFD to highlight the different particle trajectories in upward and downward facing U bends, see Figure 23, and the subsequent variation in erosion rates on each of the walls at different angular locations along the bend, see Figures 24 and 25. In the case of a downwards facing U bend (Figure 25), peak values of erosion occur at the corner of the outer and side walls at the 180° position. A smaller degree of erosion also occurs on the inner walls near the corner of the inner and side walls. In the upward facing U bend (Figure 24) erosion only occurs at the corner of the outer and side walls, although the erosion rate is much higher than in the downward facing case.

Song *et al* [20] used CFD to compare predicted erosion rates in jet pumps with different nozzle designs. Examples of the predicted fluid streamline and erosion distribution in the chosen nozzle design are shown in Figures 26 and 27. The authors concluded that CFD is a valuable tool for comparative work but suggested that relevant experimental data is needed to validate the predictions.

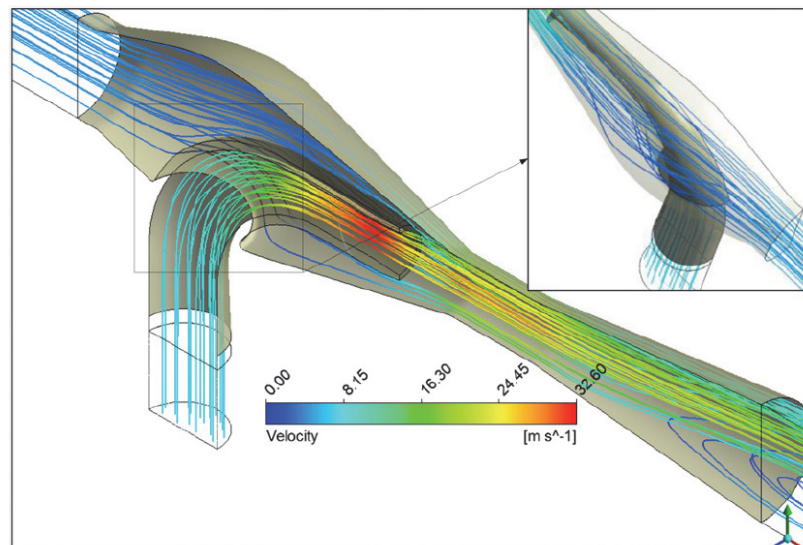


Figure 26. Fluid streamline in a jet pump [20]

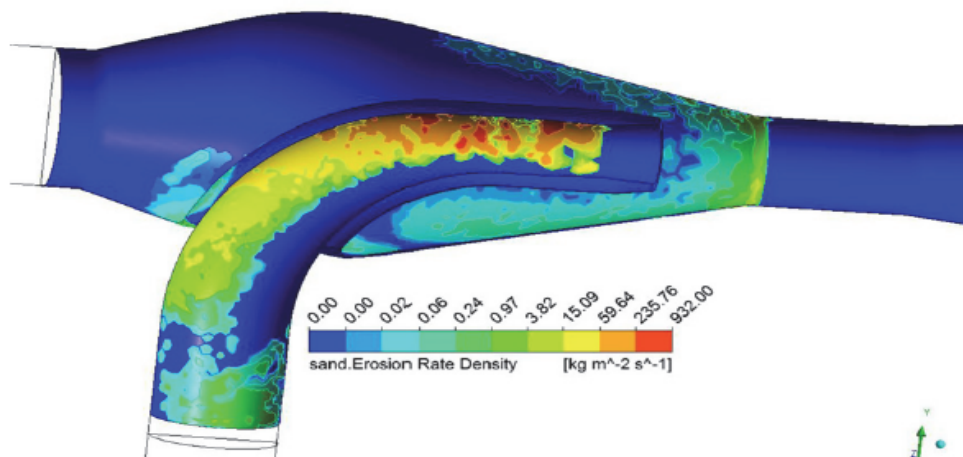


Figure 27. Erosion distribution in the jet pump [20]

5. CONCLUSIONS

Erosion is known to be a complex process that can be detrimental to industrial components with demanding in-service conditions. Experimental research carried out over many years has led to greater understanding of the erosion mechanisms. In recent years this knowledge has been applied to the development of models with the aim of predicting erosive wear.

Due to the complexity of the erosion process, no universally accepted predictive model exists. Empirical models are heavily dependent on experimental data in the form of erosion coefficients. These models are suitable for predicting erosion rates in well-defined situations where a wealth of experimental data already exists. They are useful in comparative work e.g. material ranking. If modelling of a more general erosion process or a more complex geometry is required, the empirical models are no longer applicable. For erosion of complex geometry, CFD has proven a useful tool, although this method is still reliant on erosion equations and in some cases, experimentally determined erosion coefficients. As well as dealing with complex geometries this method can also account for the effects of different types of flow.

This report has presented an overview of using CFD modelling for predicting erosive wear; concentrating on two scenarios: particulates within a gas (e.g. erosion of turbine blades) and particulates within a fluid (e.g. slurry in pipes). With CFD the computer programme performs the calculations required to simulate the interactions of liquids or gases with surfaces. This is used to predict the flow field from which the particle trajectories and hence impact velocities and impact angles can be calculated. These quantities are then input into erosion equations to calculate the erosion rate. This method is suitable for both particles/gas combinations and particle/liquid combinations and generally gives good correlation with experimental data for calculation of particle velocities and also for erosion rates.

6. REFERENCES

- [1] J. R. Nicholls, "Laboratory Studies of Erosion-Corrosion Processes Under Oxidising and Oxidising/Sulphidising Conditions," *Materials at High Temperatures*, vol. 14, no. 3, pp. 289-306, 1997.
- [2] J. Bitter, "A Study of Erosion Phenomena: Part 1," *Wear*, vol. 6, pp. 5-21, 1963.
- [3] J. F. Bell and P. S. Rogers, "Laboratory scale erosion testing of a wear resistant glass-ceramic," *Mat. Sci. Tech*, vol. 3, p. 807, 1987.
- [4] L. Dai, M. Yu and Y. Dai, "Nozzle passage aerodynamic design to reduce solid particle erosion of a supercritical steam turbine control stage," *Wear*, vol. 262, pp. 104-111, 2007.
- [5] I. M. Hutchings, "A model for the erosion of metals by spherical particles at normal incidence," *Wear*, vol. 70, pp. 269-281, 1981.
- [6] M. G. Gee, C. Phatak and R. Darling, "Determination of Wear Mechanisms by Stepwise Erosion and Stereological Analysis," *Wear*, vol. 258, pp. 412-425, 2005.
- [7] K. Tsubouchi, N. Yasugahira, S. Yoshida, R. Kaneko and T. Sato, "An Evaluation of Water Droplet Erosion for Advanced Large Steam Turbines," in *PWR Vol 10, Advances in steam turbine technology for power generation*, Boston, Massachusetts, 1990.
- [8] S. A. Shirazi, B. S. McLaury and M. M. Ali, "Sand Monitor Evaluation in Multiphase Flow," in *Proceedings of the NACE Corrosion 2000 Conference*, Orlando, USA, 2000.
- [9] I. Bargmann, A. Neville, S. Hertzman, F. Reza and X. Hu, "Erosion-Corrosion in Oil and Gas – Stainless Steel Under De-aerated Slurry Impingement Attack," in *Proceedings of the NACE Corrosion Conference*, Atlanta, USA, 2009.
- [10] M. Gustavsson, "Fluid dynamic mechanisms of particle flow causing ductile and brittle erosion," *Wear*, vol. 252, no. 11-12, pp. 845-858, 2002.

- [11] M. B. Gandhi, R. Vuthaluru, H. Vuthaluru, D. French and K. Shah, "CFD based prediction of erosion rate in large scale wall-fired boiler," *Applied Thermal Engineering*, vol. 42, pp. 90-100, 2012.
- [12] J. G. Mbabazi and T. J. Shear, "Computational prediction of erosion of air heater elements by fly ash particles," *Wear*, vol. 260, pp. 1322-1336, 2006.
- [13] M. Atkinson, E. V. Stepanov, D. P. Goulet, S. V. Sherikar and J. Hunter, "High pressure testing sand erosion in 3D flow channels and correlation with CFD," *Wear*, Vols. 270-277, p. 263, 2007.
- [14] M. A. Kuczmarski, R. A. Miller and Z. Dongming, "CFD-Guided Development of Test Rigs for Studying Erosion and Large-Particle Damage of Thermal Barrier Coatings," *Modelling and Simulation in Engineering*, no. 837921, 2011.
- [15] A. Campos-Amezcu, A. Gallegos-Munoz, C. A. Romero, Z. Mazur-Czerwicz and R. Campos-Amezcu, "Numerical investigation of the solid particle erosion rate in a steam turbine nozzle," *Applied Therm. Eng.*, vol. 27, pp. 2394-2403, 2007.
- [16] H. Zhu, Y. Lin, G. Feng, K. Deng, X. Kong, Q. Wang and D. Zeng, "Numerical analysis of flow erosion on sand discharge pipe in nitrogen drilling," *Advances in Mech Eng*, no. 952652, 2013.
- [17] S. M. El-Behery, M. H. Hamed, M. A. El-Kadi and K. A. Ibrahim, "CFD prediction of air-solid flow in 180° curved duct," *Powder Tech*, vol. 191, pp. 130-142, 2009.
- [18] C. J. Reagle, J. M. Delimont, W. F. Ng, S. V. Ekkad and V. P. Rajendran, "Measuring the coefficient of restitution of high speed microparticle impacts using a PTV and CFD hybrid technique," *Measurement Science and Technology*, vol. 24, no. 105303, 2013.
- [19] A. Keating and S. Nešić, "Numerical Prediction of Erosion-Corrosion in Bends," in *Proceedings of the NACE Corrosion 2000 Conference*, Orlando, USA, 2000.
- [20] X.-G. Song, J.-H. Park, S.-G. Kim and Y.-C. Park, "Performance comparison and erosion prediction of jet pumps by using a numerical method," *Mathematical and Computer Modelling*, vol. 57, pp. 245-253, 2013.
- [21] A. Keating and S. Nešić, "Particle tracking and erosion prediction in three-dimensional bends," in *Proc. FEDSM2000*, Boston, Massachusetts, USA, 2000.
- [22] X. Chen, B. S. McLaury and S. A. Shirazi, "Numerical and Experimental Investigation of the Relative Erosion Severity Between Plugged Tees and Elbows in Dilute Gas/Solid Two-Phase Flow," *Wear*, vol. 261, pp. 715-729, 2006.
- [23] M. Varga, C. Goniva, K. Adam and E. Badisch, "Combined experimental and numerical approach for wear prediction in feed pipes," *Tribology International*, vol. 65, pp. 200-206, 2013.
- [24] J. G. Mbabazi, T. J. Shear and R. Shandhu, "A model to predict erosion on mild steel surfaces impacted by boiler fly ash particles," *Wear*, vol. 257, pp. 612-624, 2004.
- [25] T. Frank and I. Schulze, "Numerical simulation of gas-droplet flow around a nozzle in a cylindrical chamber using a lagrangian model based on a multigrid Navier-Stokes solver," in *Int. Symp. On Numerical Methods for Multiphase Flows*, Lake Tahoe, Nevada, USA, 1994.
- [26] D. F. Fletcher, B. Guo, D. J. E. Harvie, T. A. G. Langrish, J. J. Nijdam and J. Williams, "What is important in the simulation of spray dryer performance and how do current CFD models perform?," *Applied Mathematic modelling*, vol. 30, pp. 1281-1292, 2006.
- [27] T. Schmidt, H. Assadi, F. Gartner, H. Richter, T. Stoltenhoff, H. Kreye and T. Klassen, "From particle acceleration to impact and bonding in cold spraying," *J. Thermal Spray Tech*, vol. 18, no. 5-6, pp. 794-808, 2009.
- [28] H.-Z. Li, J. Wang and J. M. Fan, "Analysis and modelling of particle velocities in micro-abrasive air jet," *J. Machine Tools & Manufacture*, vol. 49, pp. 850-858, 2009.
- [29] M. Achtsnick, P. F. Geelhoed, A. M. Hoogstrate and B. Karpuschewski, "Modelling and

- evaluation of the micro abrasive blasting process,” *Wear*, vol. 259, pp. 84-94, 2005.
- [30] B. Bozzini, M. E. Ricotti, M. Boniardi and C. Mele, “Evaluation of erosion-corrosion in multiphase flow via CFD and experimental analysis,” *Wear*, vol. 255, pp. 237-245, 2003.
 - [31] I. Finnie, “The mechanism of erosion of ductile materials,” in *Proceedings of the 3rd US Congress on Applied Mechanics*, New York, USA, 1958.
 - [32] J. G. A. Bitter, “A Study of Erosion Phenomena: Part 2,” *Wear*, vol. 6, pp. 169-190, 1963.
 - [33] P. H. Shipway and I. M. Hutchings, “Influence of nozzle roughness on conditions in a gas-blast erosion rig,” *Wear*, Vols. 162-164, pp. 148-158, 1993.
 - [34] M. Papini, D. Ciampini, T. Krajac and J. K. Spelt, “Computer modelling of interference effects in erosion testing: effect of plume shape,” *Wear*, vol. 255, pp. 85-97, 2003.
 - [35] Y. Zhang, E. P. Reuterfors, B. S. McLaury, S. A. Shirazi and E. F. Rybicki, “Comparison of Computed and Measure Particle Velocities and Erosion in Water and Air Flows,” *Wear*, vol. 263, pp. 330-338, 2007.
 - [36] A. Gnanavelu, N. Kapur, A. Neville, J. F. Flores and N. Ghorbani, “A numerical investigation of a geometry independent integrated method to predict erosion rates in slurry erosion,” *Wear*, vol. 271, pp. 712-719, 2011.
 - [37] M. Azimian and H.-J. Bart, “CFD simulation and experimental analysis of erosion in a slurry tank test rig,” *EPJ Web of Conferences*, vol. 45, p. 01009, 2013.
 - [38] M. J. Willis, T. N. Croft and M. Cross, “Computational Fluid Dynamic Modelling of an Erosion-Corrosion Test Method,” in *Proceedings of the NACE Corrosion 2009 Conference*, Atlanta, USA, 2009.
 - [39] M. M. Salama, “Influence of Sand Production on Design and Operations of Piping Systems,” in *Proceedings of the NACE Corrosion 2000 Conference*, Orlando, USA, 2000.
 - [40] D. R. Lester, L. A. Graham and J. Wu, “High precision suspension erosion modelling,” *Wear*, vol. 269, pp. 449-457, 2010.